

Electron-beam rapid quenching of an ultra high-strength alloy steel

K. J. A. MAWELLA*, R. W. K. HONEYCOMBE

Department of Metallurgy and Materials Science, University of Cambridge, Pembroke Street, Cambridge, UK

Rapid quenching using electron beams has been used to treat the surface layers of an ultra high-strength alloy steel. The microstructure of the treated surface layers has been investigated by optical, scanning and electron microscopy and by X-ray diffractometry. The microstructure produced by conventional solid state quenching of the same steel has also been examined for comparison. This microstructural study shows that the rapid quenching process leads to a high degree of grain refinement and an increase in solid solubility which, in turn, increases the amount of retained austenite. The lowering of M_s temperature due to the high cooling rate and the increased solid solubility favour the formation of twinned martensite. These interlinked phenomena have increased the microhardness of the rapidly quenched layer considerably, with respect to that of the solid state quenched steel.

1. Introduction

Rapid quenching using laser or electron beams is a method which can be used for the controlled and reproducible achievement of rapidly solidified surface layers. Since these surface layers might be expected to improve wear, erosion and corrosion resistance, numerous investigations are being carried out on the structure and properties of the rapidly quenched surfaces. Electron-beam rapid quenching involves the rapid interaction of material with a focused electron beam by traversing the beam on the material or traversing the material under the beam. This procedure yields a thin melt layer while the substrate remains cold. Rapid surface melting thus occurs in a very short time, during which a minimum amount of thermal energy is conducted to the substrate, thus giving rise to a steep temperature gradient between the solid and the liquid. Rapid solidification occurs as a result of this temperature gradient. The quench rate is mainly dependent on process parameters such as the beam power, traverse speed and the interaction time. As a result of high cooling rates, interesting metallurgical structures are produced,

which are not generally observed in solid state quenched structures.

This paper describes a microstructural investigation of electron-beam rapidly quenched surface layers of an ultra high-strength alloy steel, in which the phenomena, which cause the improvements in properties are investigated. Cooling rates have been determined using the relationship with dendrite cell sizes. The grain refinement, martensite morphology, increase in the amount of retained austenite and the increase in solid solubility are discussed. The increase in micro-hardness of the rapidly quenched region is attributed to the grain refinement and the increased solid solubility. Comparison of the microstructure with that produced by solid state quenching has also been carried out.

2. Experimental details

The steel used in this investigation had the following composition (wt %): 0.38 carbon, 0.55 manganese, 2.9 nickel, 0.7 chromium, 0.57 molybdenum, 0.23 silicon, 0.2 vanadium, balance iron. This steel had been austenitized at 980°C for 1 h before quenching in oil. Then it had been secondary

*Present address: Department of Metallurgy, University of Sheffield, Mappin Street, Sheffield, UK.

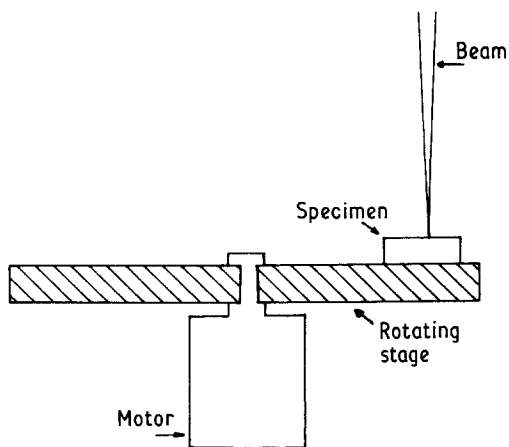


Figure 1 Schematic diagram of the electron-beam surface melting process for a specimen mounted on a rotating stage inside the vacuum chamber.

hardened and stress relieved. All the rapid quenching experiments using this steel were carried out in this as-received condition.

A modified electron-beam welding machine was used for rapid quenching. The small interaction time necessary to achieve high cooling rates was obtained by traversing the specimens under the beam. A schematic diagram of the surface melting process is shown in Fig. 1, for a specimen normally mounted on a rotating stage. The traverse speed could be varied between 4.4 cm sec^{-1} and a maximum speed of 36.4 cm sec^{-1} . Prior to the interaction with the beam, surfaces of the specimens were ground down to 180 grit finish. No coatings were applied for the absorption of power, since the electron beam to material energy transfer efficiency was high enough to melt the surfaces.

For comparative purposes, solid state quenched

specimens of the same steel were produced from 1 mm thick strip, which were austenitized at 1473 K for 1 h and quenched in iced brine.

Specimens for optical microscopy were prepared from both materials and 2% Nital was used as the etchant. Thin foil specimens for transmission electron microscopy were ion-beam thinned and were examined in a Philips EM 300 electron microscope. An ISI 100 scanning electron microscope was used to take micrographs for dendrite cell measurements.

The lattice parameter measurements were obtained by X-ray diffractometry using $\text{CoK}\alpha$ radiation. A Leitz micro-hardness tester was used with a 0.1 kg load to measure the microhardness.

3. Results

In the transverse and longitudinal cross-sections (Fig. 2) of rapidly quenched steel, the melt and heat-affected zones were readily distinguished from the substrate. Since the re-solidified region consisted of a highly refined microstructure, it was difficult to clearly observe details by optical microscopy. The martensitic nature of the steel after melting and resolidifying is clearly distinguishable in the scanning electron micrographs of the melted region. As an example, a region melted with a beam power of 50 W and a traverse speed of 29.6 cm sec^{-1} is shown in Fig. 3. It was observed that the thin area marked "a" in Fig. 3, adjacent to the heat-affected zone was on a particularly refined scale similar to a chilled zone of a solidifying ingot. From this region columnar dendrites grew into the melt. Apart from the columnar dendrites, the rapidly quenched region also showed a cellular structure, which consisted of cross-sections of the dendrites grown parallel to the path of the

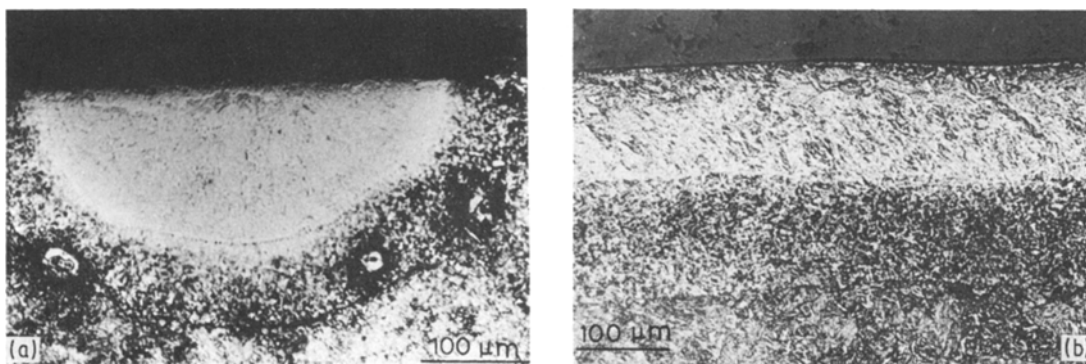


Figure 2 Optical micrographs of (a) transverse and (b) longitudinal cross-sections of the regions rapidly quenched using a beam power of 100 W and a traverse speed of 4.4 cm sec^{-1} .

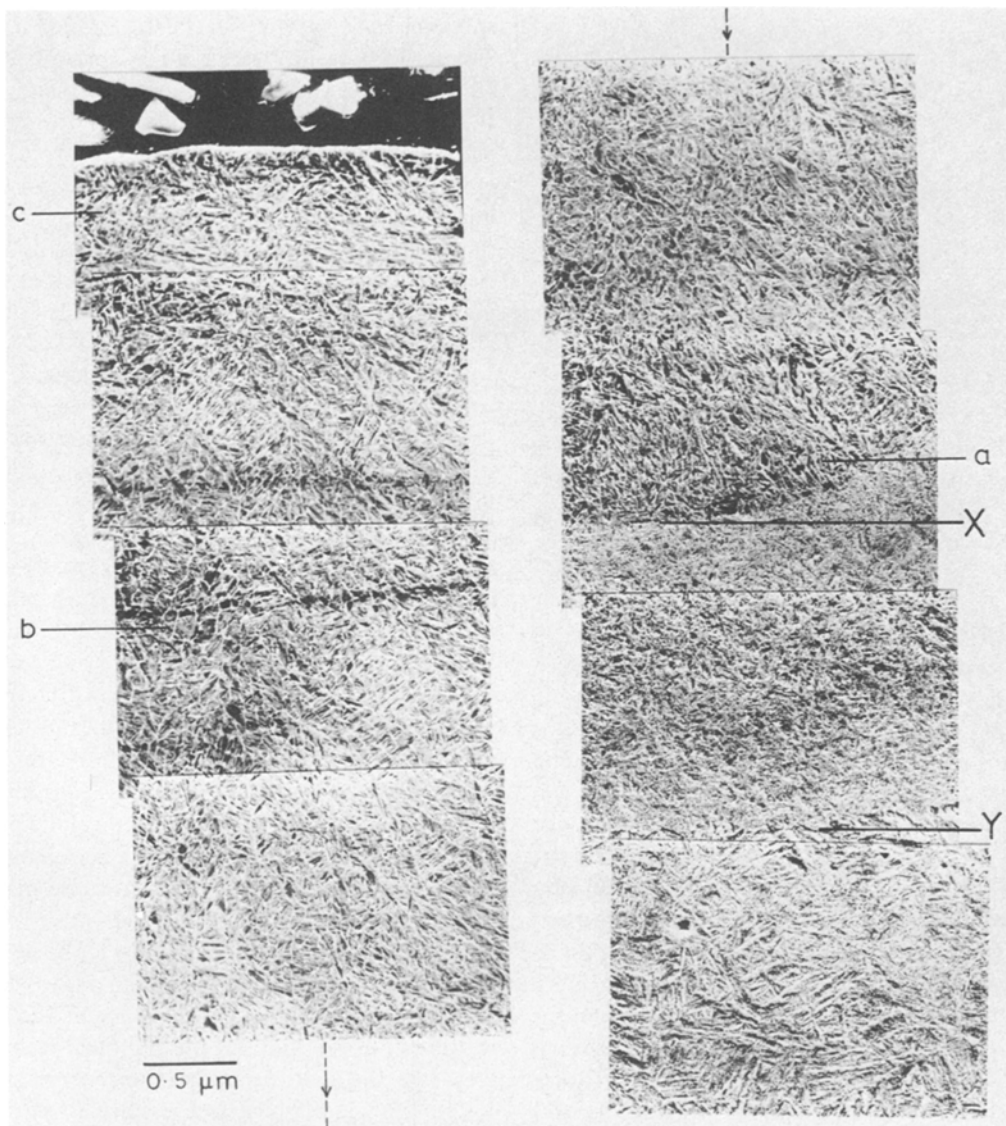


Figure 3 Scanning electron micrograph of a transverse cross-section of an area, rapidly quenched using a beam power of 50 W and a traverse speed of 29.6 cm sec^{-1} . (Only a strip from the surface to the substrate is shown here.) X and Y indicate the ends of solidified and heat-affected zones.

beam due to the temperature gradient in that direction.

The solid state quenched sample exhibited prior austenite grains, which contained differently oriented packets of martensite lathes. The average grain size was about $75 \mu\text{m}$. Figs. 4 and 5 are optical micrographs of solid state quenched and rapidly quenched samples, respectively. The rapidly quenched structure appeared to consist of martensite plates less than $3 \mu\text{m}$ wide. The effect of the cooling rate on the microstructure is also shown in Figs. 5a and b which are the microstruc-

tures of steel, rapidly quenched using the same traverse speed but with beam powers of 100 and 1200 W, respectively. Calculations [1] have shown that the increasing beam power at a constant speed decreases the cooling rate. It is observed that the average size of martensite plates and the width of the columnar dendrites decrease as the beam power is reduced.

By using transmission electron microscopy, the electron-beam rapidly quenched microstructures were found to consist mainly of dislocated martensite. Fig. 6 is an example of the plate structure

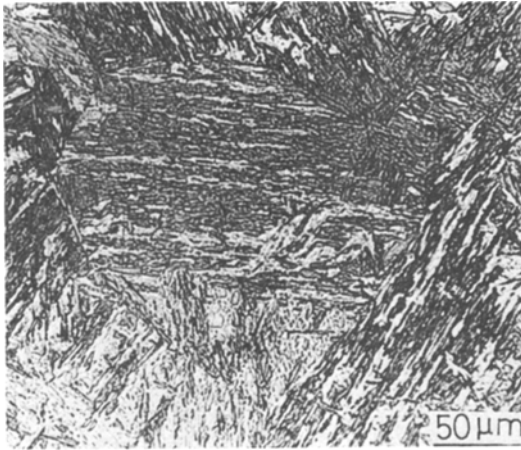


Figure 4 An optical micrograph of the structure of solid state quenched steel.

observed. The apparent width of these plates varied from 100 nm to about 250 nm. The martensite plates were often twin oriented and a large proportion of the plates was internally twinned. Fig. 7 shows the very fine internal twins (apparent widths of some of the twins 10 nm) found in a martensite plate in the surface-melted steel. In solid state quenched structures, only a very few internal twins were found.

Retained austenite was detected as interlath films in electron-beam quenched structures. Fig. 8 is a 002_{γ} centred dark-field electron micrograph showing some of the retained austenite observed. The X-ray diffractometer traces of solid state quenched and completely electron-beam melted steel surfaces are shown in Figs. 9a and b. No

austenite peaks were detected in the solid state quenched steel, but the rapidly quenched structures gave rise to small austenite peaks, indicating an increase in the amount of austenite retained by electron-beam surface quenching.

Electron microscopy did not reveal any significant quantities of carbides in the rapidly quenched structures. Fig. 10 shows the variation of microhardness with the depth below the surface in the rapidly quenched region. The microhardness of the steel substrate was only 350 VPN, but it increased to about 810 to 820 VPN, when rapidly quenched. The microhardness of the solid state as quenched steel was about 460 VPN.

4. Discussion

4.1. Cooling rate

In the microstructures of electron beam rapidly quenched steel, a variation of the dendrite spacing was observed. In the particular region shown in Fig. 3, the average cell diameter near the surface was about $0.4 \mu\text{m}$ (area c), while the average cell diameter of the area in the middle of the melt pool (area b) was about $0.75 \mu\text{m}$. According to the relationship between the dendrite spacing, d , and the cooling rate, r , derived by Matyja *et al.* [2]:

$$dr^a = c \text{ (where } a \text{ and } c \text{ are constants),}$$

the measured dendrite spacings correspond to cooling rates of $2 \times 10^6 \text{ }^\circ\text{C sec}^{-1}$ at the surface and $2.4 \times 10^5 \text{ }^\circ\text{C sec}^{-1}$ in the middle of the quenched region. The trend of decreasing cooling rate with the depth below the surface is in agreement with calculations [1].

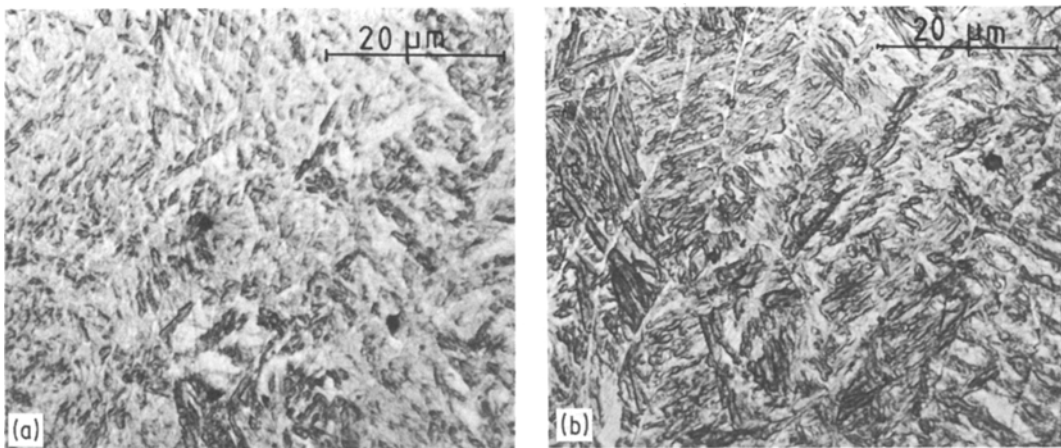


Figure 5 Microstructure of steel, rapidly quenched using a traverse speed of 4.4 cm sec^{-1} and beam powers of (a) 100 W and (b) 1200 W (SEM).

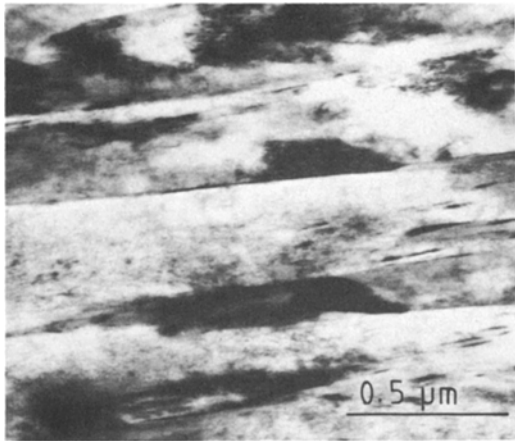


Figure 6 Martensitic microstructure in electron beam surface melted region (TEM).

4.2. Grain refinement

Although it was not possible to determine the prior austenite grain sizes of the rapidly quenched structure, it is clear that the average size of martensite units in the rapidly quenched structure is smaller than that of the solid state quenched structure. Since the austenite grain size determines the maximum size of a martensite plate, it is reasonable to assume that the electron-beam treated steel structure consisted of prior austenite grain sizes much smaller than those in the solid state quenched structures.

Grain refinement is a phenomenon which occurs in rapid quenching and is not dependent on the method used to obtain the rapidly quenched structure. For example, the refinement of the

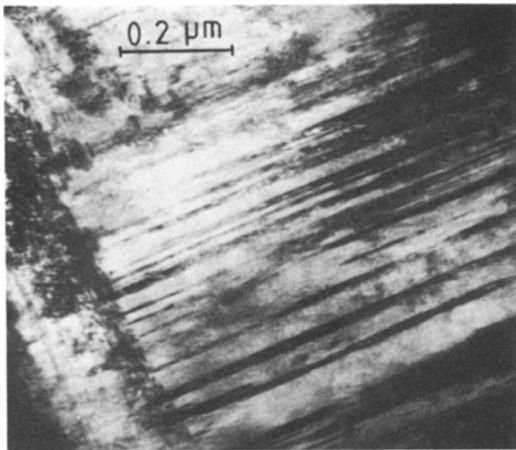


Figure 7 Internal twins in an electron beam surface melted region (TEM).

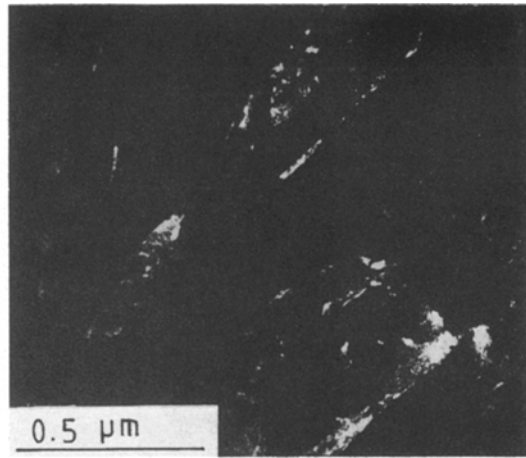


Figure 8 A 002_{γ} centred dark-field electron micrograph showing retained austenite in electron-beam rapidly quenched structure.

grain size in melt-spun ultra high-strength alloy steel was reported earlier by the present authors [3]. There is strong support for the view that the high rate of quenching determines the fine grain size. Based on a homogeneous nucleation solidification model, Boswell and Chadwick [4] demonstrated a strong dependence of grain diameter, d_1 , on the cooling rate at the melting point R :

$$d_1 = 1.75 \times 10^7 R^{-0.9}.$$

Refinement of grain size is one of the important strengthening mechanisms in the heat treatment of steels (Hall–Petch relationship [5]), which must account for part of the increase in strength caused by rapid quenching, as reflected in the microhardness of the rapidly quenched steel which was much higher than that of the solid state quenched steel.

4.3. Martensite morphology

The presence of many fine twins in the electron-beam quenched structure indicated that rapid quenching favours the formation of twinned martensite plates. It seems that the martensite morphology does not depend on the process used for rapid quenching, as melt-spun ribbons of the same steel also contained heavily twinned martensite plates [3]. This change in the martensite morphology can be attributed to the influence of the very high cooling rate on the martensite transformation temperature (M_s) which, in fact, is related to the critical resolved shear stress (CRSS) for slip and twinning. In iron base alloys, the M_s temperature has been found to be depressed by

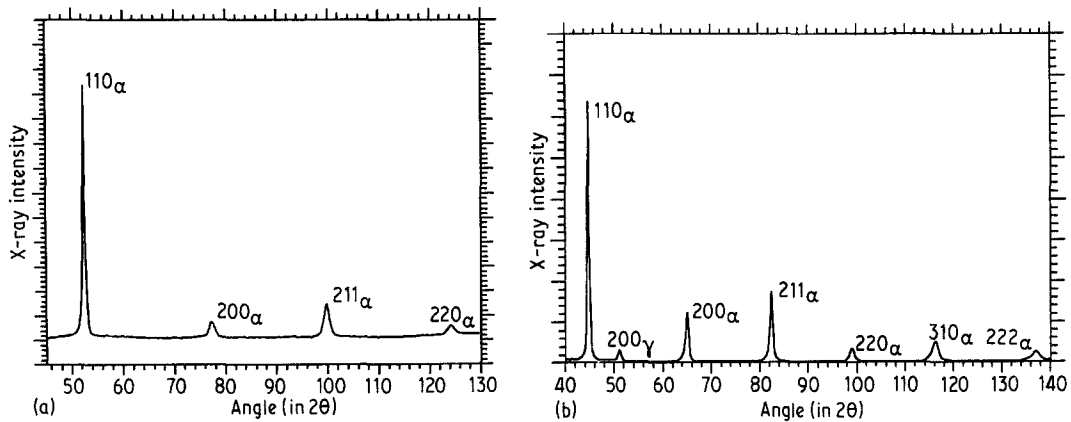


Figure 9 X-ray diffractometer traces of (a) solid state quenched steel ($\text{CoK}\alpha$ radiation), (b) completely electron-beam melted surface of steel ($\text{CuK}\alpha$ radiation).

high cooling rates [6, 7]. Also Thomas [8] showed that high cooling rates increased the solid solubility by inhibiting the alloy carbide precipitation, and this increase in the solute content in turn lowered the M_s temperature. During rapid quenching, at the lowered M_s temperature, the CRSS for twinning becomes lower than that for slip, reversing the behaviour at higher temperatures. Consequently, the lattice invariant part of the martensitic transformation occurs preferentially by twinning rather than by slip.

4.4. Solid solubility

As mentioned in the earlier section, the high cooling rates inhibit the carbide nucleation and growth. In the present work, this was confirmed by the observed lack of autotempering. The measurement of the lattice parameters of martensite in electron-beam quenched and solid state quenched steel showed that the inhibition of carbide precipitation

leads to a greater supersaturation (Table I). It can be seen that even after allowing for the practical errors in measurement, the lattice parameter of electron-beam quenched steel is greater than that of the solid state quenched steel, implying a higher carbon concentration in the martensite lattice of rapidly quenched steel.

4.5. Retained austenite

The increase in the amount of retained austenite, which occurs during rapid quenching is caused by the increased solid solubility of the alloying elements and the grain refinement. When the carbides and other elements are dissolved in solid solution, an increase in the retained austenite would occur since the elements are free to stabilize austenite. This would be reflected in a depression of the M_s temperature, which is also depressed by the high cooling rate employed with the overall result that more austenite is retained. The austenite is further stabilized by closely spaced boundaries (fine grains) due to the minimization of growth of martensite after nucleation as has been demonstrated previously by Leslie and Miller [9].

5. Conclusions

1. Electron-beam rapidly quenched regions of ultra high-strength steel consisted of columnar and cellular dendrites. Cooling rates up to $2 \times 10^6 \text{ }^\circ\text{C}$

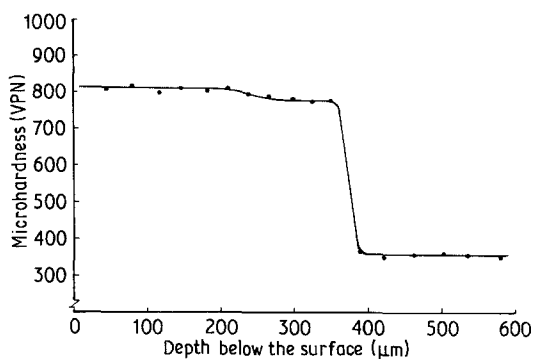


Figure 10 Variation of microhardness with the depth below the surface in an electron-beam melted region of steel (beam power = 200 W, traverse speed = 4.4 cm sec⁻¹).

TABLE I

Condition	Average lattice parameter (nm)
Solid state quenched	0.28690 ± 0.00014
Electron-beam quenched	0.28794 ± 0.00044

sec⁻¹ were found to occur during rapid solidification.

2. The rapid quenching process led to a high degree of grain refinement.

3. Inhibition of alloy carbide precipitation led to higher solid solubility.

4. The increased amount of twinning in the rapidly quenched martensite is attributed to the lowering of the M_s temperature, since it is the preferred mode of lattice invariant shear at lower temperatures.

5. The increased solid solubility and the grain-refinement effect have resulted in an increase in the amount of retained austenite.

6. Interlinked phenomena such as austenite grain refinement, the increased solubility and the mainly martensitic structure have led to a large increase in micro-hardness.

Acknowledgement

The authors acknowledge financial support from the Procurement Executive, Ministry of Defence.

References

1. K. J. A. MAWELLA, PhD thesis, University of Cambridge (1983).
2. H. MATYJA, B. C. GIESSEN and N. J. GRANT, *J. Inst. Metals* 96 (1968) 30.
3. K. J. A. MAWELLA, R. W. K. HONEYCOMBE and P. R. HOWELL, *J. Mater. Sci.* 17 (1982) 2850.
4. P. G. BOSWELL and G. A. CHADWICK, *Scripta Metall.* 11 (1967) 459.
5. N. J. PETCH, *JISI (Lond.)* 174 (1953) 25.
6. R. C. RUHL and M. COHEN, *Trans. Met. Soc. AIME.* 245 (1969) 253.
7. Y. INOKUTI and B. CANTOR, *Scripta Metall.* 10 (1976) 655.
8. G. THOMAS, *Met. Trans.* 2 (1971) 2373.
9. W. C. LESLIE and R. L. MILLER, *Trans. ASM* 57 (1964) 972.

Received 23 January

and accepted 30 January 1984